

# Field test corrosion experiences when co-firing straw and coal: Ten year status within Elsam

Rasmus B. Frandsen<sup>1</sup>, Melanie Montgomery<sup>2</sup>, Ole Hede Larsen<sup>1</sup>

## Abstract

In Denmark, straw is utilised for the generation of energy and district heating in power plants. Combustion of straw gives rise to high contents of potassium chloride and some sulphur dioxide in the flue gas. These compounds can lead to deposits with high content of potassium chloride and potassium sulphate on superheater tubes resulting in increased corrosion rates. From field experimental results this paper shows, that by co-firing straw with coal, corrosion rates can be brought down to an acceptable level.

This paper firstly deals with the results from a demonstration program co-firing coal and straw at the 150 MW pulverized coal fired boiler Studstrup unit 1. Two exposure series lasting 3000 hours each were performed for co-firing 10 and 20 % of straw (% energy basis) with coal. Using built in test tubes in the hot end of the actual superheaters and air/water cooled corrosion probes, the corrosion during these experiments was monitored. Various ferritic and austenitic materials were investigated at steam temperatures ranging from 520 – 580 °C and flue gas temperatures ranging from 925 – 1100 °C.

The results obtained in the demonstration program led to the rebuilding of the 350 MW pulverized coal fired boiler, Studstrup unit 4, into a co-firing boiler with straw in 2002. During the rebuilding, test tube sections of X20CrMoV12 1 and TP347H FG were built into the superheater and the reheater loops. The temperature ranges during these exposures was for the steam from 470 – 575 °C and for the flue gas from 1025 – 1300 °C. All these test tubes have been removed during the last three years at one year intervals for corrosion studies.

The corrosion studies performed on all investigated tubes included measurements of the corrosion attack, light optical microscopy and scanning electron microscopy of the corrosion products.

## 1. Introduction

The motivation for using straw as a fuel for the production of heat and power is that it is regarded as carbon dioxide neutral, and therefore provides abatement of CO<sub>2</sub> emissions.

It is well established [1] that when combusting straw significant amounts of sulphur dioxide and potassium chloride will be introduced into the flue gas. Through condensation and deposition processes these components will result in the formation of superheater deposits rich in potassium chloride and potassium sulphates, which gives rise to different degrees of accelerated corrosion.

The corrosiveness of straw combustion products limits the possibility for high efficiencies as steam temperatures must be kept relatively low so as not to introduce rapid corrosion rates of the hottest components such as superheaters. The reason for this is that the main corrosion mechanism, chlorination, has a very high degree of temperature dependence [2]

<sup>1</sup> Elsam Engineering, Kraftværksvej 53, 7000 Kolding, Denmark.

<sup>2</sup> IPL/Energi E2/Elsam Technical University of Denmark, Building 204, Kemitorvet, 2800 Lyngby, Denmark.

As an alternative to pure straw firing, Elsam, in 1996 started a demonstration program on co-firing. Trials with up to 20% straw (% energy basis) were undertaken in the pulverised coal fired boiler Studstrup unit 1. The main conclusion regarding depositions and corrosion mechanism in this work was, compared with pure straw firing, that co-firing leads to reduced depositions of potassium chloride and a greater emission of hydrogen chloride gas (although still below the acceptable emissions level). A sequestering mechanism was proposed where the potassium chloride from the straw reacts with the minerals from the coal to form non-corrosive potassium aluminosilicates and the chlorine is released as hydrogen chloride gas.

In fact, the overall results from the demonstration program were so encouraging that the 350 MW pulverised coal fired boiler Studstrup unit 4 was rebuilt for co-firing in 2002 and later in 2005 the 350 MW sister boiler Studstrup unit 3 was also rebuilt.

The present paper will briefly review the results from the demonstration program. Then results gained from built-in test tubes in the superheaters and reheater in Studstrup unit 4 will be addressed and compared with the results from the demonstration project.

## 2. Experimental

A range of different superheater materials were tested during the demonstration project and results have been given elsewhere [4,5]. X20CrMoV121 and TP347H FG were chosen for testing in Studstrup unit 4 and for purposes of comparison only results from these materials will be presented. The nominal chemical compositions of these two materials are given in table 1.

Table 1 Nominal chemical composition in wt% of investigated steel (balance Fe)

	C	Cr	Ni	Mo	Si	Mn	V	Nb
X20CrMoV121	0.17 - 0.23	10.00 - 12.50	0.30 - 0.80	0.80 - 1.20	< 0.50	<1.00	0.25 - 0.35	
TP347H FG	0.04 - 0.10	17.00 - 20.00	9.00 - 13.00		< 0.75	< 2.00		0.80 - 1.00

After exposure, rings were cut from the specimens and these were mounted by vacuum impregnation of epoxy resin. The mounted cross-sections were ground and polished according to normal preparation techniques but without the use of water as a lubricant. The extent of corrosion attack, corrosion products and ash deposits were investigated using light optical microscopy and scanning electron microscopy with energy dispersive X-ray analysis.

### 2.1 Studstrup unit 1

The demonstration program was conducted on the 150 MW power plant Studstrup unit 1, now demolished, which had been modified for co-firing straw. The unit had main steam data of 160 bar/540°C at the superheater outlet and 43 bar/540 °C at the reheater outlet section. The steam flow is from platen superheater to superheater 2 to turbine to reheater.

Two trial series each lasting approx. 3000 hours were conducted, where 10 % straw (energy basis) and 20 % straw (energy basis) were used as fuels. The coal type was a Columbian type classified as a low corrosive coal. During these trials high temperature corrosion was investigated on both air-cooled corrosion probes and test superheater sections which were welded into the existing superheaters. The result from the tubes built into the superheater sections reflects the corrosion rates that would be encountered with the plants present operation parameters. The chosen set temperatures for the probes ranged from those in the plant to a steam temperature of 580 °C. Tests were conducted both in areas with modest steam temperature and high flue gas temperature and in areas with high steam temperature and lower flue gas temperature. This was undertaken to observe how different combinations steam/flue gas temperature influences ash deposits and corrosion rates. An overview of the combination of experimental parameters is given in table 2.

Table 2 Overview of the experimental parameters investigated during the demonstration project.

Sample type	Corrosion probes				Test tube sections	
Sample name	K1a,b	K2a,b	K3a,b	K4a,b	4, 9, 3	7, 8, 6
Position	2 <sup>nd</sup> SH	2 <sup>nd</sup> SH	2 <sup>nd</sup> SH	Plat SH	2 <sup>nd</sup> SH	Plat SH
Flue gas Temp. °C	925	925	925	1100	925	1100
Steam Temp. °C	520	550	580	500-530	540	475
Metal Temp. °C - 10% straw	556	580	612	550	565	525
Metal Temp. °C - 20% straw	541	563	586	588	565	525
Exposure time hr. - 10%straw	2540	2770	2770	2770	300	3000
Exposure time hr. - 20%straw	2980	3012	3012	3012	3012	3012

## 2.2 Studstrup unit 4

Studstrup unit 4 has since 2002 been co-firing app. 10% straw (energy basis) with coal. The unit has main steam data of 250 bar/540°C at the superheater outlet and 49 bar/560 °C at the reheater outlet section. The steam flow is from superheater 3 to superheater 4 to turbine to reheater.

Corrosion was investigated by exposing test sections in the actual superheater and reheater loops. The first parts of these sections were removed after 1 year exposure (7231 hrs) with an average straw share of 7.5%. The second parts were removed after 2 years (17719 hrs) with an average straw share of 9.8% and the last part of these test tubes were removed after 3 years (22597 hrs) with an average straw share of 9.3%. The location of the test sections were in superheater 3, superheater 4 and in the reheater. Table 3 gives an overview of the conducted experiments.

Superheater 3 has an inlet steam temperature of 380°C and an outlet steam temperature of 550°C. Since the tube investigated was midway between the inlet and outlet, the steam temperature has been estimated to be 465°C. The temperature may be slightly higher than this due to the heat flux to which this outer loop is exposed. The flue gas temperature before superheater 3 is 1220°C.

Superheater 4 has an overall outlet steam temperature of 540°C. However the actual outlet steam temperature of tube 18 where the test section was located is 575°C as measured in the penthouse. Since the test section is close to the outlet, it is assumed that this has a similar steam temperature. The flue gas temperature before superheater 4 is 1020°C.

For the reheater tube investigated, the outlet steam temperature is 560°C and since the test section is close to the outlet, it is assumed that it has a similar steam temperature. The flue gas temperature before the reheater is 940°C.

Table 3 Overview of the experimental parameters investigated at Studstrup unit 4

Position	Superheater 3			Superheater 4			Reheater		
	1.1- 1.2	1.3 - 1.4	1.5 - 1.6 - 1.7	2.1	2.2	2.3	3.1	3.2	3.3
Sample name									
Flue gas Temp. °C	1220	1220	1220	1020	1020	1020	940	940	940
Steam Temp. °C	465	465	465	575	575	575	560	560	560
Metal Temp. °C	485	485	485	595	595	595	580	580	580
Straw share %	7.5	9.8	9.3	7.5	9.8	9.3	7.5	9.8	9.3
Exposure time hr.	7231	17719	22597	7231	17719	22597	7231	17719	22597

Sample 1.2, 1.4, 1.6 are TP347H FG, remaining samples are X20CrMoV121

## 3. Results

The results section will only briefly review the results from the demonstration project as they have been published and discussed in a number of other publications [3, 4, 5]. Hereafter the newly obtained results

from Studstrup unit 4 will be shown in detail. These results will then be compared and discussed with the results from the demonstration project in the discussion section.

### 3.1 Studstrup unit 1

#### 3.1.1 Corrosion products

The main elements detected in the ash attached to the corrosion products are aluminium, silicon, sulphur, potassium, calcium and iron. Whilst aluminium and silicon decrease as the percentage of straw in fuel increases, the percentage of sulphur and potassium increases. Virtually no chlorine was detected in the deposits or corrosion product. The composition of the ash was particles rich in aluminium, silicon, potassium and oxygen in a matrix rich in potassium, sulphur and oxygen, i.e. potassium sulphate.

For both 10% and 20% straw, thick two-layered oxides were formed on X20CrMoV121, also some evidence of broad pits have been observed see. figure 1. The inner layer was rich in chromium and the outer layer was an iron oxide with, in many cases, fly-ash particles incorporated into the surface of the outer layer. Sulphur has been detected at the inner-outer layer interface or within the inner oxide layer, generally up to  $3 \pm 4$  wt.% but sometimes as high as 13 wt.%. For X20CrMoV121, generally thick oxide scales were seen however very occasionally thin ( $1 \mu\text{m}$ ) chromium rich scales were observed.

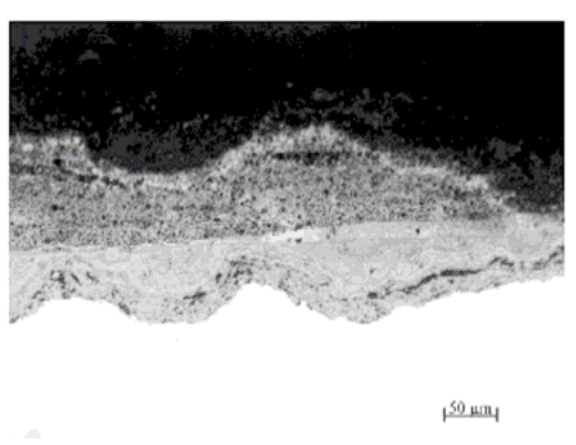


Figure 1 X20CrMoV121 probe 2 metal temperature 563°C with 20% straw co-firing

For TP347H FG, there was a tendency for formation of thin oxide of  $1 \mu\text{m}$  or thick broad pits where there was a chromium rich inner oxide layer and an iron rich outer oxide layer. In addition needles of haematite were present within the deposit adjacent to the oxide. The deposit consisted of round particles, which were silicon and aluminium rich. Sulphur and chromium, presumably as chromium sulphide, were found in the inner corrosion product close to the corrosion front. There was nickel enrichment in the metal adjacent to the corrosion front. The metal at the corrosion front was porous, perhaps due to the fast diffusion of iron and chromium leaving vacancies behind. The thin oxide consisted of chromium rich oxide with an outer layer of iron oxide. Thus for TP347H FG if a chromium layer does not form initially, then a duplex oxide layer is formed.

### 3.2 Studstrup unit 4

#### 3.2.1 Corrosion Products

The main constituent of the deposits adjacent to the corrosion products on all samples was aluminium, silicon, calcium, sulphur, potassium and iron. In some instances especially in the reheater section the thickness and composition of the deposits varied greatly with flue gas direction. High concentrations of potassium were, in most cases associated with high concentrations of sulphur indicating the presence of potassium sulphate. Chlorine was only detected in the fly ash on a few occasions.

For the X20CrMoV121 samples in superheater 3, double layered oxides were formed. The inner oxide layer was enriched in chromium while the outer oxide layer was a pure iron oxide in which fly ash particles were incorporated. After all exposure times, minor amounts of sulphur were detected in the inner oxide indicating the presence of sulphides or sulphates. Sulphur was also detected at the corrosion front but there was no evidence of appreciable internal attack.

For the austenitic TP347H FG tubes in superheater 3, double layered oxides were formed. The inner oxide layer was enriched in chromium while the outer oxide layer was a pure iron oxide which had fly ash particles incorporated. Compared with X20CrMoV121 samples both the inner and the outer oxide layers were much thinner. In some isolated areas the inner oxide layer was only 2 – 3  $\mu\text{m}$  thick even after 22597 hours of exposure. Sulphur in the presence of sulphides or sulphates were detected in the oxide layers as well as at the corrosion front. Evidently more sulphur rich internal attack was experienced for these samples as compared to the X20CrMoV121 samples that had been exposed to the same conditions Figure 1.

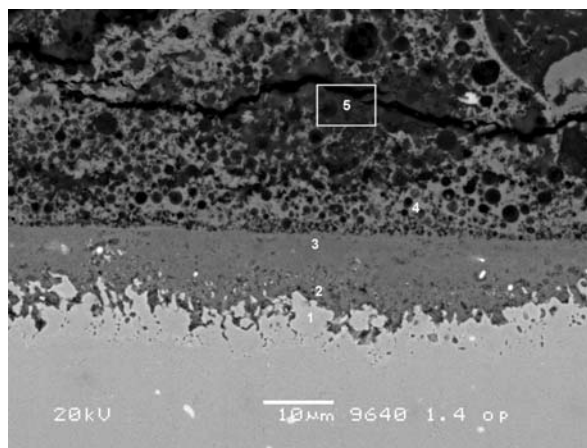


Figure 2 TP347H FG exposed for 17719 hours in superheater 3 showing minor amount of internal attack.

Only the martensitic X20CrMoV121 material was exposed in superheater 4. All investigated samples showed an inner and an outer oxide where the inner oxide was rich in chromium and the outer oxide was an iron oxide. After all exposure times, sulphur, present as sulphides or sulphates were detected in the oxide layers as well as at the corrosion front as depicted in figure 3. Severe internal corrosion attack in the form of sulphidation was observed at grain boundaries to a depth of 40  $\mu\text{m}$  already after 7231 hours of exposure. The depth of the internal corrosion attack stayed constant over time while the chromium rich inner oxide layer grew in size. EDS spot analysis performed on samples exposed for 17719 hours showed sulphur content in the internal attack zone of up to 47 at%. Internal attack areas very high in sulphur were always associated with high amounts of chromium and/or iron and no oxygen clearly indicating the presence of iron/chromium sulphides - figure 2b.

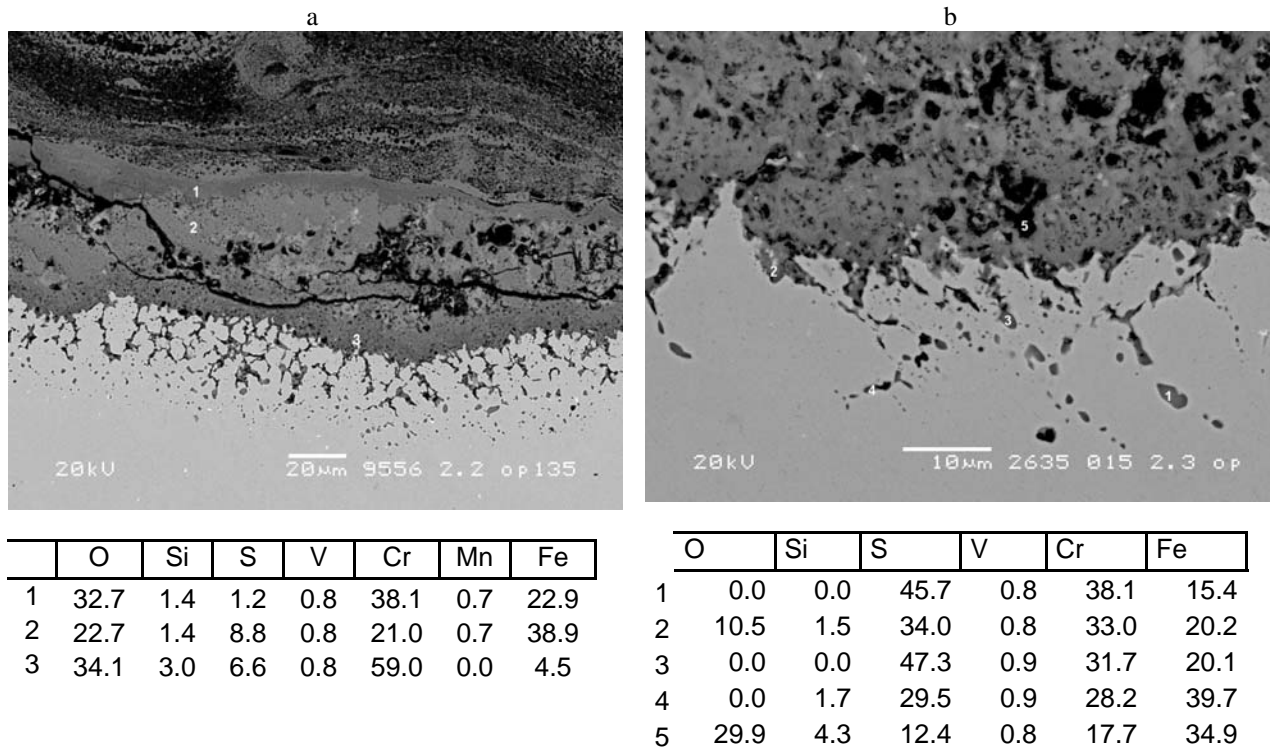


Figure 3 X20CrMoV121 exposed in superheater 4 for 17719 hours showing internal attack. EDS in at%

In addition, the bulk metal area of the internal attack zone suffered from severe chromium depletion. Consequently a poor oxidation resistance of this area is to be expected. This might explain the observed growth rate for the inner oxide layer after longer exposure times.

Reheater samples after 7231 hours showed a double layered oxide. Very thin oxide layers were occasionally found on the opposite side of flue gas direction. On the flue gas direction side internal grain boundary attacks, rich in sulphur and metallic alloying elements, i.e. sulphides, were observed to a depth of approx. 25 µm. After 17719 hours of exposure a very interesting observation was made as shown in figure 4. Here chlorine appeared at the corrosion front and the inner chromium rich oxide layer was in these areas very thick. As it can be seen from figure 3 there is an unexpected low chromium content at the corrosion front associated with chlorine and an unexpected high chromium content in the outer oxide layers. This could suggest that chromium is evaporating from the corrosion front as  $\text{CrCl}_2(\text{g})$  and then migrates out of the metal due to its high volatility to areas of a higher oxygen partial pressure where it is converted to chromium oxide and chlorine.

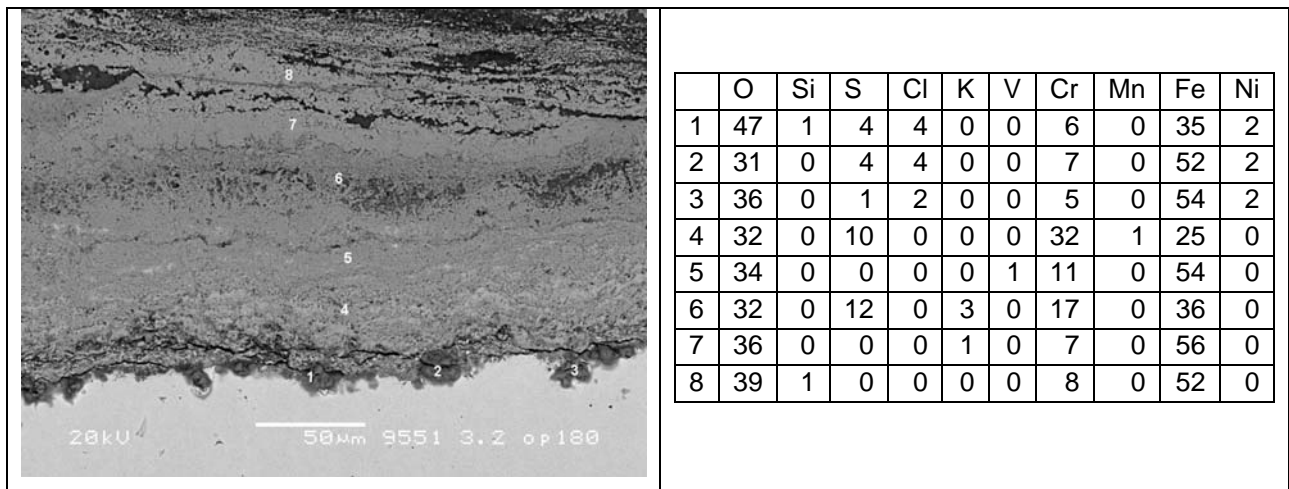


Figure 4 X20CrMoV121 reheater sample exposed for 17719 hours showing chloride attack. EDS at%

Surprisingly the samples after 22597 hours did not show any sign of chlorine at the corrosion front. Here the corrosion morphology was the same as after 7231 hours of exposure. The inner oxide was enriched in sulphur and there was the presence of sulphides with some internal sulphur attack at the corrosion front. Sulphides of chromium and iron were present, and in some cases manganese. Also there was chromium depletion in the matrix at the corrosion front where internal sulphur attack had occurred.

## 4. Discussion

### 4.1.1 Corrosion rates

The corrosion rates for X20CrMoV121 for the experiments from unit 4 are compared with results from the demonstration project. They have been plotted in an Arrhenius type plot and are depicted in figure 5 assuming a parabolic corrosion rate according to equation 1. Here  $x$  is the thickness of the inner chromium rich oxide layer including internal attack and  $t$  is the duration of exposure. Thus the logarithm of the parabolic rate constant is plotted as a function of the reciprocal time.

$$x^2 = 2 \cdot k_p \cdot t \quad (1)$$

It can be observed from figure 5 that the corrosion rates are higher than would be expected compared to the results from the demonstration project. A possible reason is that 3000 hours of exposure is too short a time to get a reliable idea of the corrosion rates after long exposure time. This could be further supported by the general trend observed for the samples exposed at Studstrup unit 4 where corrosion rates after 22597 hours are all higher than corrosion rates after 7231 hours. More internal attack is observed on the samples from Studstrup unit 4 than on the samples from the demonstration project, which may indicate that after longer exposures, there is a greater concentration of sulphur in the corrosion product which leads to internal sulphidation at the corrosion front. Internal sulphidation after longer exposure times has also been observed at Avedøre II, where there is co-firing of heavy oil + gas + wood pellets. Internal sulphidation was not observed in the first two years but in the 3<sup>rd</sup> year after 19,000 hours exposure[14]

The reheater sample from the exposure duration 17719 hours is anomaly showing a high corrosion rate. This is interesting when remembering that it was in this sample chlorine was detected at the corrosion front. Just as interesting is it that the corrosion rate decreases again after 22597 hours. This supports the fact that no chlorine was found in this sample and indicates clearly that the presence of chlorine results in an increased corrosion rate compared to sulphidation.

Generally the corrosion rates for the X20CrMoV121 samples increases as the metal temperature increases.

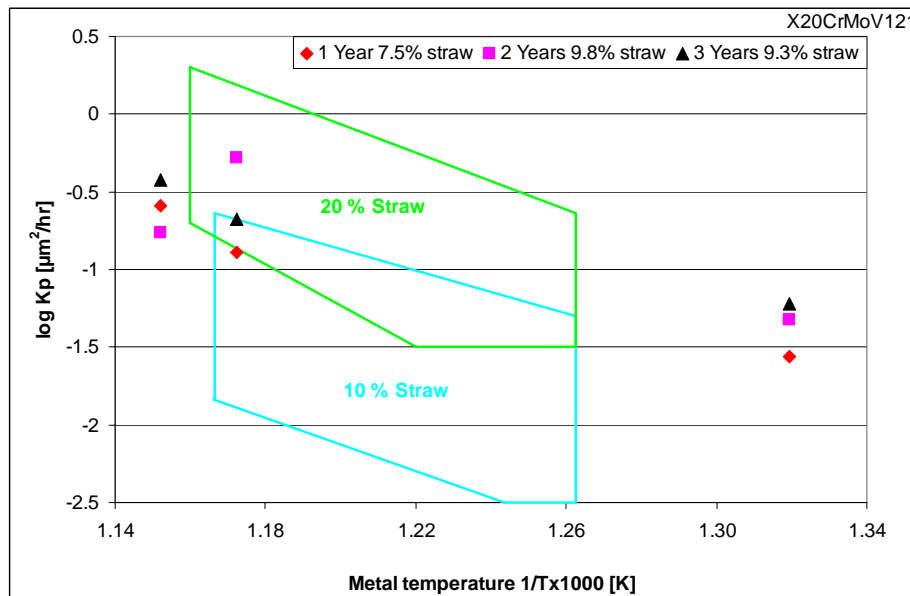
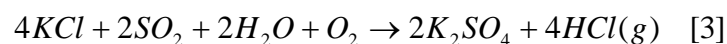
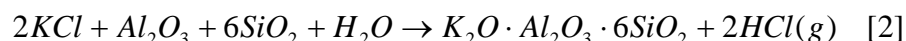


Figure 5 Arrhenius plot showing corrosion constant of X20CrMoV121 when co-firing straw and coal.

#### 4.2 Corrosion products

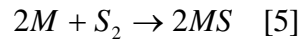
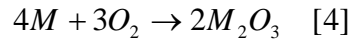
For all specimens investigated, with the exception of the reheater sample after 2 years, there were no signs of chlorine induced corrosion and no signs of potassium chloride in the deposits. Thus, the overall conversion mechanism of potassium chloride proposed by Montgomery et.al [3] on specimens from the demonstration program also fits with the newly obtained results. This mechanism suggests that when co-firing coal and straw, straw introduced potassium chloride either reacts to form non corrosive potassium aluminosilicates or reacts to form potassium sulphates. With both reaction routes HCl gas is released into the flue gas in accordance with equation 2 and 3 below.



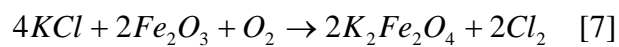
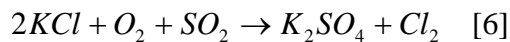
Of these reaction products it is the presence of the potassium sulphate that will induce corrosion when deposited on the metallic components.

Generally the presence of potassium sulphate will, depending of the actual metal temperature give rise to two different corrosion mechanisms. These mechanisms are either sulphidation or hot corrosion by the more complex alkali-metal trisulphates. Analysis of the corrosion products showed that sulphur in the form of sulphates and sulphides are present within the corrosion products. The presence of metal oxides such as iron oxide needles within a sulphate deposit is not observed as was the case in some of the higher temperature specimens with 20% straw co-firing from the demonstration project. Thus, the corrosion mechanism consists primarily of oxidation together with sulphidation. Many workers [6,7,8,9] have investigated sulphidation in gaseous environments where SO<sub>2</sub>, SO<sub>3</sub> or S<sub>2</sub> migrates through the oxide scale via vacancies or micro cracks to form sulphides at the corrosion front or within the metal preferentially at grain boundaries. In pure coal firing the presence of sulphides at the oxide-metal interface has also been reported [10]. On the basis of the above observations it is therefore suggested for the recent

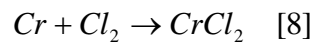
co-firing experiments presented here that sulphidation and oxidation occur according to equation 4 and 5 (M being Fe or Cr) where the oxidants are supplied from potassium sulphates present in the deposits.



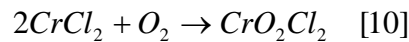
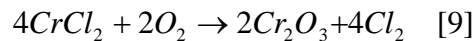
The reheater sample after 2 years was the only sample which showed signs of chlorine induced corrosion. This indicates that some amount of potassium chloride has been present in the deposit and has reacted to form potassium sulphate or potassium ferrate and chlorine gas according to equation 6 and/or 7.



The released chlorine then migrates through the protective oxide to react, preferentially with Cr, at the metal-oxide interface equation 8.



The chromium chloride formed then migrates out of the metal due to its high volatility to areas of a higher oxygen partial pressure where it is converted to chromium oxide and chlorine equation 9. In addition chromium chloride can also react with oxygen to produce chromium oxychloride which has a high volatility equation 10.



Chlorine then migrates back to the corrosion front to form metal chlorides again. This corrosion mechanism is known as active oxidation where chlorine has an almost catalytic role in converting the metal to its oxide [12].

Since chlorine was not detected at the metal-oxide interface in the sample exposed for 3 years, chlorine must be able to evaporate out of the system described by equation 5 and 6. Thus, given time with no new supply of chlorine there will ultimately be an infinitely small chlorine content at the metal-oxide interface. Salmenoja [13] investigated the effect of corrosion for Fe-Cr alloys in HCl at 600-700°C after the HCl supply was stopped. A memory effect of 20 minutes was shown before the corrosion rate decreased to its original level before the introduction of chlorine. Since the conditions in Salmenoja's work are so different from Studstrup, it is not possible to estimate the duration of the memory effect. However, the results presented here and Salmenoja's work show that corrosion with chlorine containing substances will decrease with time when the source of chlorine is stopped and will not perpetually affect the system.

The presence of chlorine in the specimen gives higher corrosion and it indicates that at some point in time not all the potassium chloride has reacted in the combustion chamber, and therefore has deposited on the reheater. This indicates how vulnerable the system is due to occasional irregularities that may occur during operation.

Comparing the results from the demonstration project with the newly obtained results with much longer exposure times, it is suggested that the basic corrosion mechanism given in the demo project is in good agreement with the corrosion mechanism observed here. The morphology of the oxide layers is compa-

rable but a larger amount of internal attack is observed compared with the demonstration project. Reasons for this should most likely be sought in the longer exposure times, which give more reliable results and also the fact that two different boilers have been utilized will introduce uncertainties.

## **5. Conclusion**

From this investigation on co-firing approx. 10% straw with coal the following conclusions can be drawn. The corrosion rates observed are a higher level than what would have been expected from the results obtained in the demonstration project. Still, corrosion rates are much lower than those measured in pure straw fired boilers. In the two year reheater sample chlorine was detected at the corrosion front. This leads to an increase in the corrosion rate but, chlorine had disappeared in the three year sample and the corrosion rate fell to a much lower level.

On all other components investigated the main corrosion mechanism is sulphidation, which results in sulphides and sulphates within the oxide layer, and internal attack preferentially at grain boundaries at the corrosion front. With exception of the internal attack, the corrosion mechanism is the same as that observed with 10 % straw in the demonstration project

It should be emphasised that the results presented here are extremely dependent on coal and biomass type. If a coal contains less aluminium and silicon, then the alkali capture could be less efficient leading to either greater deposition of potassium sulphate and possible deposition of potassium chloride. If a coal had high sodium content, this could lead to deposition of sodium sulphate which would reduce the temperature that low temperature hot corrosion would occur.

## **6. Acknowledgement**

Part of this research has been funded by Eltra PSO R&D programme

## 7. References

- [1] B. Sander, K. W. Hansen, 14th European Biomass Conference, Paris, 2005
- [2] M. Montgomery, A. Karlsson, O. H. Larsen, EUROCORR2000, London, 2000
- [3] M. Montgomery, O. H. Larsen Materials and Corrosion 53, 2002, 185
- [4] M. Montgomery, O. H. Larsen, O. Biede CORROSION/2003, paper 03356
- [5] M. Montgomery, O. H. Larsen EUROCORR2000, London, 2000
- [6] F. Gesmundo, D. J. Young, S. K. Roy, High Temp. Materials and Processes 8, 1989, 149
- [7] K. Tjokra, Ph.D Thesis, New South Wales, 1992
- [8] T Narita, Proc. International Symposium on High Temperature Oxidation and Sulphidation Processes, Hamilton, Ontario, Canada, 1990
- [9] H. J. Grabke, Materials at High Temperatures Volume 11, 1993
- [10] J. L. Blough, Proc. NACE Conference CORROSION/88, paper 129
- [11] S. C. Srivastava, K. M. Godiwalla, M. K. Banerjee, Journal of Material Science 32, 1997, 835
- [12] H. J. Grabke, E. Reese, M. Spiegel, Corrosion Science 37, 1995, 1023
- [13] K. Salmenoja, Ph.D. Thesis, Åbo Akademi, Finland 2000
- [14] M. Montgomery et al Poster to presented at Liege.